



TITLE:

Disturbed hippocampal intra-network in first-episode of drug-naïve major depressive disorder

AUTHOR(S):

Watanabe, Keita; Okamoto, Naomichi; Ueda, Issei; Tesen, Hirofumi; Fujii, Rintaro; Ikenouchi, Atsuko; Yoshimura, Reiji; Kakeda, Shingo

CITATION:

Watanabe, Keita ...[et al]. Disturbed hippocampal intra-network in first-episode of drug-naïve major depressive disorder. *Brain Communications* 2023, 5(1): fcac328.

ISSUE DATE:

2023

URL:

<http://hdl.handle.net/2433/285137>

RIGHT:

© The Author(s) 2022. Published by Oxford University Press on behalf of the Guarantors of Brain.; This is an Open Access article distributed under the terms of the Creative Commons Attribution License, which permits unrestricted reuse, distribution, and reproduction in any medium, provided the original work is properly cited.

BRAIN COMMUNICATIONS

Disturbed hippocampal intra-network in first-episode of drug-naïve major depressive disorder

 Keita Watanabe,¹ Naomichi Okamoto,² Issei Ueda,³ Hirofumi Tesen,² Rintaro Fujii,² Atsuko Ikenouchi,² Reiji Yoshimura² and Shingo Kakeda³

Complex networks inside the hippocampus could provide new insights into hippocampal abnormalities in various psychiatric disorders and dementia. However, evaluating intra-networks in the hippocampus using MRI is challenging. Here, we employed a high spatial resolution of conventional structural imaging and independent component analysis to investigate intra-networks structural covariance in the hippocampus. We extracted the intra-networks based on the intrinsic connectivity of each 0.9 mm isotropic voxel to every other voxel using a data-driven approach. With a total volume of 3 cc, the hippocampus contains 4115 voxels for a 0.9 mm isotropic voxel size or 375 voxels for a 2 mm isotropic voxel of high-resolution functional or diffusion tensor imaging. Therefore, the novel method presented in the current study could evaluate the hippocampal intra-networks in detail. Furthermore, we investigated the abnormality of the intra-networks in major depressive disorders. A total of 77 patients with first-episode drug-naïve major depressive disorder and 79 healthy subjects were recruited. The independent component analysis extracted seven intra-networks from hippocampal structural images, which were divided into four bilateral networks and three networks along the longitudinal axis. A significant difference was observed in the bilateral hippocampal tail network between patients with major depressive disorder and healthy subjects. In the logistic regression analysis, two bilateral networks were significant predictors of major depressive disorder, with an accuracy of 78.1%. In conclusion, we present a novel method for evaluating intra-networks in the hippocampus. One advantage of this method is that a detailed network can be estimated using conventional structural imaging. In addition, we found novel bilateral networks in the hippocampus that were disturbed in patients with major depressive disorders, and these bilateral networks could predict major depressive disorders.

1 Open Innovation Institute, Kyoto University, Kyoto 6068501, Japan

2 Department of Psychiatry, University of Occupational and Environmental Health, Kitakyushu 8078555, Japan

3 Department of Radiology, Graduate School of Medicine, Hirosaki University, Hirosaki 0368502, Japan

Correspondence to: Keita Watanabe

Open Innovation Institute, Kyoto University

216 Kokusai Kagaku Innovation, Yoshidahonmachi

Sakyo-ku, Kyoto-shi, Kyoto-fu, Japan

E-mail: watanabe.keita.2x@kyoto-u.ac.jp

Keywords: hippocampal network; structural covariance network; hippocampus; major depression

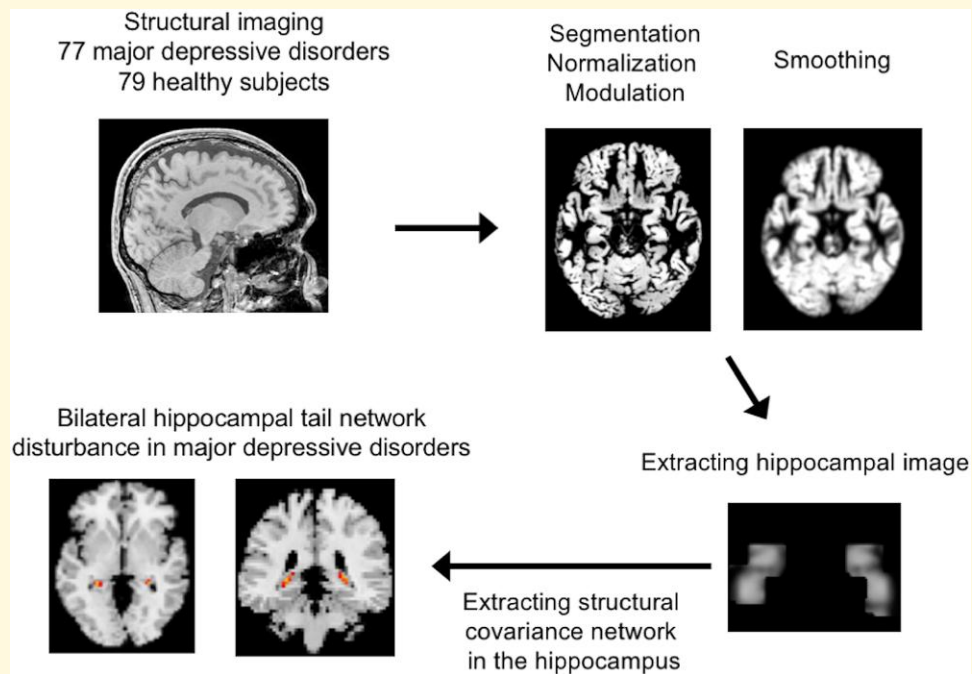
Abbreviations: CA = cornu ammonis; DARTEL = diffeomorphic anatomical registration through exponential Lie Algebra; DSM-IV-TR = diagnosis and statistical manual for mental disorders, fourth edition text revision; GM = grey matter; HAMD-17 = 17-item Hamilton Rating Scale for Depression; HSs = healthy subjects; IC = independent component; ICA = independent component analysis; MANCOVA = multivariate analysis of covariance; ROC = receiver operating characteristic; SBM = source-based morphometry; SCID = structured clinical interview for DSM-IV-TR; SPSS = Statistical Package for the Social Sciences; VBM = voxel-based morphometry

Received March 14, 2022. Revised September 27, 2022. Accepted December 06, 2022. Advance access publication December 8, 2022

© The Author(s) 2022. Published by Oxford University Press on behalf of the Guarantors of Brain.

This is an Open Access article distributed under the terms of the Creative Commons Attribution License (<https://creativecommons.org/licenses/by/4.0/>), which permits unrestricted reuse, distribution, and reproduction in any medium, provided the original work is properly cited.

Graphical Abstract



Introduction

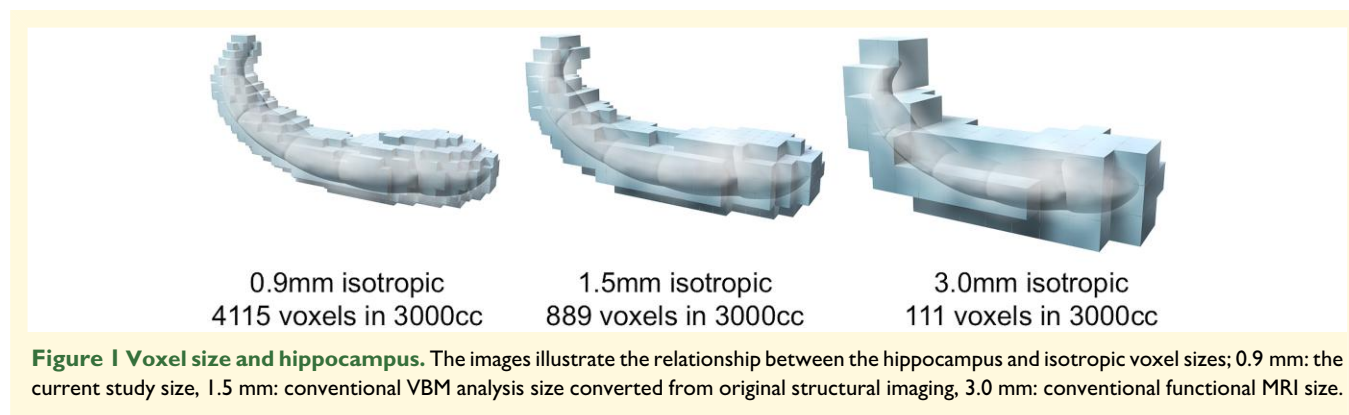
The hippocampus is thought to play an important role in major depressive disorder. Previous meta-analyses have revealed a reduction in hippocampal volume in major depressive disorder.¹⁻³ Furthermore, reduced hippocampal volume may be associated with the risk of major depressive disorder⁴ and the severity of depressive symptoms.⁵

In terms of network topology, the hippocampus has been characterized as a hub, exhibiting structural covariance with multiple other brain regions in keeping with its central role in multiple cognitive processes.⁶ In contrast, there exists a complex network inside the hippocampus.⁷ To evaluate intra-networks, previous studies used resting-state functional MRI and hippocampal subfield segmentation techniques.^{8,9} However, there are highly discrepant segmentation protocols for hippocampal subfield segmentation.¹⁰ In addition, even with a high-resolution setting, the resolution of resting-state functional MRI may not support hippocampal subfield segmentation.^{11,12} Therefore, it is not easy to depict the intra-networks in the hippocampus from resting-state functional MRI.

To evaluate the network across the brain using MRI, structural imaging was used as the structural covariance network, in addition to functional MRI and diffusion tensor imaging. Structural covariance networks arise due to neural plasticity; regions that fire and wire together might also be coupled in particular volumes because of mutually trophic and plasticity-related changes at the synaptic and cellular levels.¹³ Although not identical, the structural covariance networks are

thought to allow the evaluation of brain networks in a way similar to resting-state functional MRI such as default mode network¹⁴ and basal ganglia network.¹⁵ Compared with the grey matter (GM) volume analysis using voxel-based morphometry (VBM), the structural covariance network analysis can improve sensitivity to detect the GM differences in psychiatric disorders.¹⁶ Furthermore, in multi-site structural imaging analysis, the structural covariance network can reduce noise and scanner effects.¹⁷ In addition, structural imaging has the advantage of a high spatial resolution, which is considered important for evaluating the hippocampus. For instance, with a total volume of 3 cc, the hippocampus contains 3000 voxels for a 1 mm isotropic voxel size of conventional structural imaging or ~111 voxels for a 3 mm isotropic voxel of conventional functional or diffusion tensor imaging (Fig. 1). Therefore, we hypothesized that information on the detailed intra-network of the hippocampus could be extracted by utilizing the high spatial resolution of structural imaging. The structural images of patients with psychiatric disorders have been accumulated in numerous studies and evaluating the intra-network of the hippocampus from structural imaging may greatly advance the understanding of brain abnormalities in psychiatric disorders.

To evaluate the intra-network in the hippocampus, we combined the advantages of high spatial resolution of conventional structural imaging and structural covariance networks. We aimed to extract the intra-network in the hippocampus using the high spatial resolution of conventional original structural imaging and investigate intra-network abnormalities in patients with major depressive disorders.



Materials and methods

Participants

All human experiments were performed in accordance with the guidelines provided and approved by the Institutional Review Board of the University of Occupational and Environmental Health School of Medicine, Japan (approval number: H25-13). All participants provided written informed consent to participate in this study.

This study included 77 first-episode drug-naïve patients with major depressive disorder and 79 healthy subjects (HSs). All subjects had participated in our previous study¹² that had analysed the whole-brain structural network using conventional source-based morphometry (SBM). A well-trained psychiatrist diagnosed patients with major depressive disorders using a fully structured clinical interview for diagnosis and statistical manual for mental disorders, fourth edition text revision (DSM-IV-TR) (SCID) between March 2009 and July 2018. Furthermore, patients with major depressive disorders were required not to have previously met the criteria for any DSM-IV-TR Axis I disorder. In addition, only patients with a 17-item Hamilton Rating Scale for Depression (HAM-D-17) score ≥ 14 , mild to moderate or higher severity,¹⁸ were eligible for inclusion in the study.

The psychiatrist excluded patients with a history of neurological disease or the presence of either Axis I (schizophrenia, other affective disorders, and so on) or Axis II (personality disorders, mental retardation, and so on) psychiatric disorders. In total, 79 HSs were recruited from nearby communities through an interview conducted by the same psychiatrist using the full SCID-I, non-patient edition. None of the HSs had a history of serious medical or neuropsychiatric illnesses or a family history of major psychiatric or neurological illnesses among their first-degree relatives. Detailed information is described in a previous study.¹²

MRI acquisition

A 3T MRI system (Signa EXCITE 3T; GE Healthcare, Waukesha, WI, USA) was used for MR images of three-dimensional fast-spoiled gradient-recalled acquisition. An

eight-channel brain phased-array coil was equipped. We set the acquisition parameters as follows: repetition time, 10 ms; echo time, 4.1 ms; inversion time, 700 ms; flip angle, 10°; matrix, 256 × 256; field-of-view, voxel size, 0.9 × 0.9 × 1.2 mm. After zero-interpolation filling, the recon parameters were as follows: recon matrix 512 × 512; recon voxel size, 0.47 × 0.47 × 0.6 mm. We corrected image distortions and intensity inhomogeneity using the Grad Warp software program¹⁹ and ‘N3’ function,²⁰ respectively. MRI parameter is also described in a previous study.¹²

Image processing

The process of conventional VBM analyses with SPM12 software (Statistical Parametric Mapping 12; Institute of Neurology, London, UK)^{21,22} was used for pre-processing of images. The structural images in native space were spatially normalized, segmented into GM, white matter and cerebrospinal fluid images, and modulated using the Diffeomorphic Anatomical Registration Through Exponential Lie Algebra (DARTEL) toolbox in SPM12.²³ DARTEL is considered as an accurate method for normalization.²¹ In contrast to conventional VBM processing, to maintain high spatial resolution, the voxel size was set at 0.9 mm isotropic voxel size, which is normally converted to a 1.5 mm isotropic voxel size.

Furthermore, the resulting modulated GM images were smoothed using a 3 mm full width at half maximum Gaussian kernel. After the smoothing process, we extracted the hippocampal image defined by automated anatomical labelling²⁴ using the WFU PickAtlas version 3.0.4.^{25,26} Figure 2 shows the process flow.

To identify structural networks among hippocampal voxels, SBM analysis was performed using the group independent component analysis (ICA) of functional MRI toolbox (<http://icatb.sourceforge.net>).¹⁶ The minimum description length principle suggested nine reliable independent components (ICs). We performed ICA using a neural network algorithm (Infomax) that attempts to minimize the mutual information of the network outputs to identify naturally grouping and maximally independent sources.²⁷ ICA was repeated 20 times to investigate the reliability of ICA estimates of ICASSO²⁸ to ensure the stability of the estimated

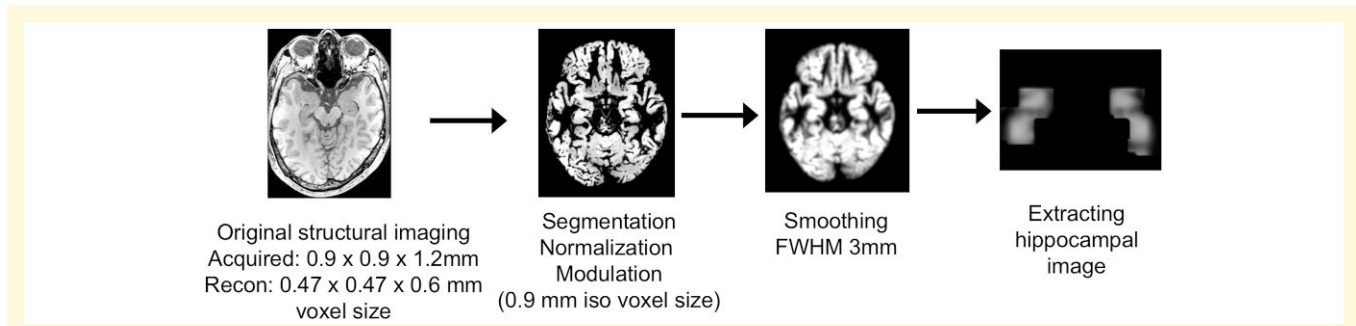


Figure 2 Image processing flow. The image processing applied Conventional VBM analysis using SPM 12. Voxels of the hippocampus were extracted. To maintain high-resolution, the voxel size was set as 0.9 mm isotropic in the normalization process, and a 3 mm full width at half maximum Gaussian kernel was used in the smoothing process.

Table 1 Demographic data

	MDD (n = 77)	HS (n = 79)	P value
Age, mean (range, SD)	52.0 (22–73, 15.1)	38.9 (20–65, 10.2)	<0.01
Female, numbers	44	34	0.08
Years of education, mean (SD)	13.4 (2.5)	16.7 (3.0)	<0.01
HAMD-17, mean of total scores (SD)	22.6 (5.9)		

HAMD-17 = 17-item Hamilton Rating Scale for Depression; MDD = major depressive disorders; SD = standard deviation.

components as in earlier works.^{29–32} We selected the mode of RandInit. The min and max cluster size was set as 16 and 20, respectively.

As a result, a matrix showed the 156 rows of 156 subjects (79 HS and 77 major depressive disorder). Columns indicate a voxel. ICA decomposed the matrix into two matrices. The first matrix comprises a subject per row and an IC per column. This matrix involves loading coefficients that show how each IC contributes to the 156 subjects. Therefore, this matrix includes data on the relationship between each subject and each IC. The loading coefficients reflect the expression of specific brain structural covariance networks for each subject. The second matrix specifies the relationship between the ICs and the voxels.

To visualize the ICs, the source matrix was reshaped back to a three-dimensional image, scaled to unit standard deviations (*Z* maps), and the threshold at $|z| > 3.0$.

Statistical analysis

Statistical analyses were conducted using Statistical Package for the Social Sciences (SPSS; version 27.0, IBM Corp., Armonk, NY, USA). Differences were considered statistically significant at $P < 0.05$. In the analysis of multivariate analysis of covariance (MANCOVA) and binominal logistic regression analysis, a threshold of <0.007 using Bonferroni correction was applied to find components showing a significant effect of diagnosis from seven components.

To compare the demographic characteristics between patients with major depressive disorder and HSs, a two-tailed *t*-test was performed to assess differences in age and years of education. The χ^2 test was used for sex comparisons. In the MANCOVA analysis, the diagnosis group (HS and major depressive disorder) was entered as an independent variable, while all loading coefficients were calculated to indicate intra-network connectivity in the hippocampus. Age, sex and years of education were used as covariates. In addition, binominal logistic regression analysis was used to assess whether the intra-networks in the hippocampus could predict major depressive disorder. To confirm whether major depressive disorder can be predicted from only MRI information, only the loading coefficients of networks were used as predictive variables, and age and gender were not used. A receiver operating characteristic (ROC) curve analysis was also performed based on the prediction formula of the logistic regression analysis. Results

Baseline demographic data

Table 1 shows the baseline demographic data of the participants. There were significant differences in age and years of education between HSs and major depressive disorders, but there were no significant differences between the sexes.

Intra-network in hippocampus

The ICA analysis generated nine ICs. Two experienced neuroradiologists reviewed these components. The anatomical regions of the hippocampal subfields were determined based on an illustrated tutorial research paper³³ with the consent of neuroradiologists. Two of these components were determined to be artefacts based on the criteria defined by Xu *et al.*:¹⁶ components containing several sharp edges near the boundary of the brain or those appearing primarily in regions that do not contain GM. These components were excluded from the subsequent analyses. Figure 3 and Table 2 show the ICs representing the structural covariance networks in the hippocampus. The two characteristics were as

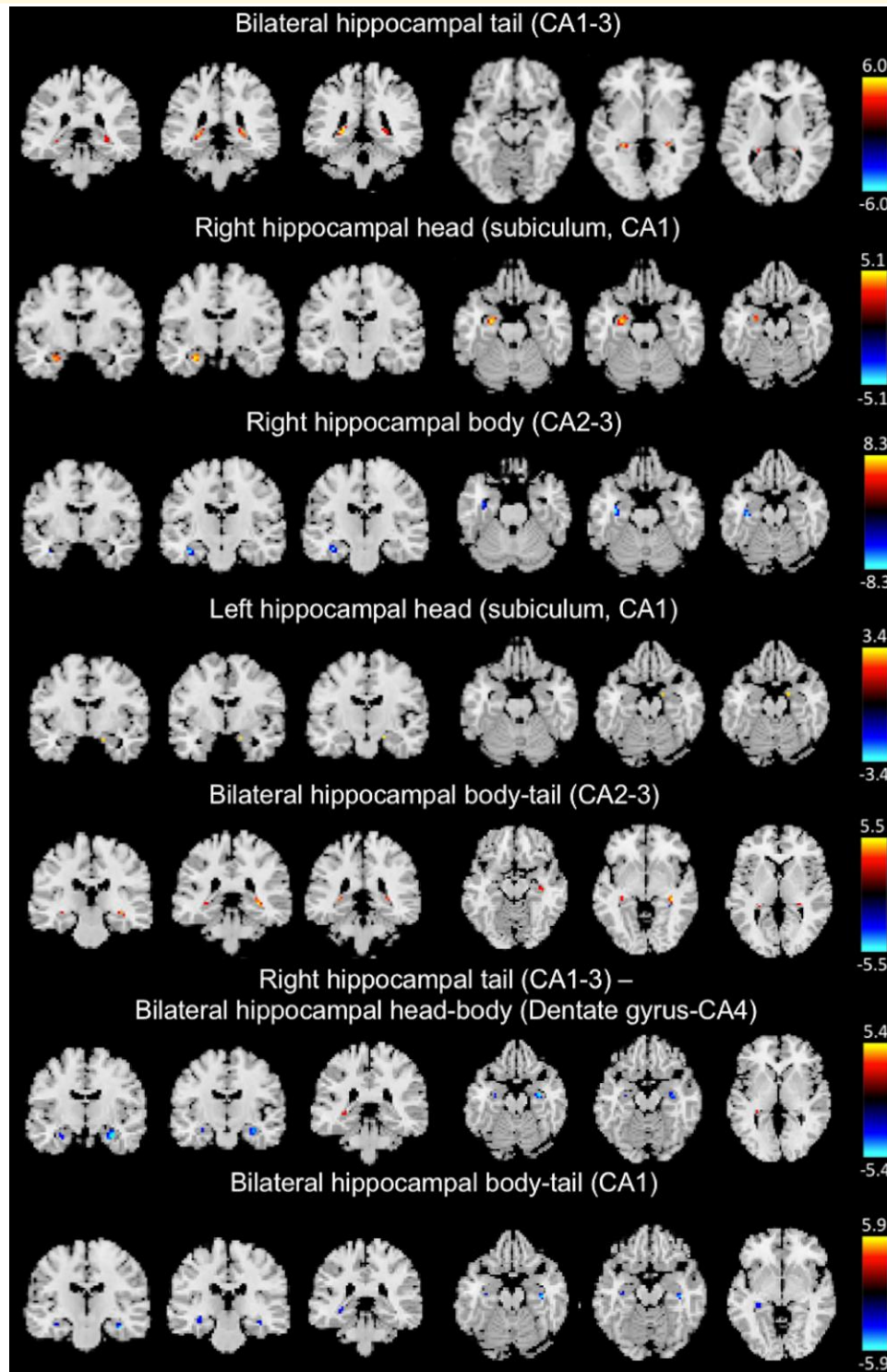


Figure 3 Voxel-based structural covariance intra-network in the hippocampus. The figures show the structural covariance networks with $|Z| > 3.0$. Red/yellow: voxel volumes show a positive correlation. Blue/light blue: the voxel volumes show a negative correlation.

follows: bilateral networks [bilateral hippocampal tail (cornu ammonis: CA1–3), bilateral hippocampal body–tail (CA2–3), right hippocampal tail (CA1–3), bilateral hippocampal head–body (dentate gyrus-CA4), bilateral

hippocampal body–tail (CA1)] and networks along the longitudinal axis [bilateral hippocampal tail (CA1–3), right hippocampal body (CA2–3) and bilateral hippocampal body–tail (CA2–3)].

Table 2 Intra-networks in hippocampus

Anatomical regions of structural covariance network	Volume (cc) left/ right	Max z-value for left/right hemisphere (Talairach coordinates x, y, z)
Bilateral hippocampal tail (CA1–3)	0.3/0.4	7.3 (–25, –38, 2)/5.8 (28, –36, 2)
	0.3/0.1	6.0 (–22, –38, 5)/5.2 (25, –36, 5)
Right hippocampal head (subiculum, CA1)	0.6/0.0	5.6 (–26, –10, –22)/0 (0, 0, 0)
	0.2/0.0	4.4 (–23, –9, –22)/0 (0, 0, 0)
	0.3/0.0	3.1 (–23, –6, –19)/0 (0, 0, 0)
	0.2/0.1	3.2 (–36, –27, –12)/2.6 (26, –45, 4)
Right hippocampal body (CA2–3)	0.8/0.0	9.4 (–37, –17, –18)/0 (0, 0, 0)
	0.4/0.1	8.2 (–36, –14, –20)/2.8 (34, –8, –25)
Left hippocampal head (subiculum, CA1)	0.1/0.6	2.7 (–20, –16, –14)/3.5 (20, –15, –15)
	0.0/0.3	0 (0, 0, 0)/2.8 (20, –2, –21)
	0.1/0.0	2.9 (–26, –10, –23)/0 (0, 0, 0)
Bilateral hippocampal body–tail (CA2–3)	0.3/0.7	4.4 (–29, –35, 2)/5.6 (33, –32, –1)
	0.2/0.1	3.3 (–33, –27, –6)/4.2 (29, –33, 4)
	0.0/0.2	0 (0, 0, 0)/2.8 (37, –25, –14)
Right hippocampal tail (CA1–3)–bilateral hippocampal head– body (dentate gyrus-CA4)	0.3/0.0	3.4 (–30, –34, 0)/0 (0, 0, 0)
	0.1/0.3	3.1 (–30, –11, –19)/5.6 (32, –11, –20)
	0.1/0.6	3.4 (–26, –10, –23)/5.5 (27, –9, –23)
Bilateral hippocampal body–tail (CA1)	0.2/0.0	3.4 (–36, –36, –9)/0 (0, 0, 0)
	0.1/0.4	3.3 (–35, –20, –15)/6.4 (38, –18, –18)
	0.4/0.3	4.3 (–33, –30, –7)/6.2 (37, –14, –19)

Table presents max z-value and Talairach coordinate of areas with a volume of 0.1 cc or more.

Table 3 Differences between MDD and HS using a MANCOVA analysis

	F	ηp^2	P
Bilateral hippocampal tail (CA1–3)	8.53	0.05	0.004*
Right hippocampal head (subiculum, CA1)	1.36	0.01	0.25
Right hippocampal body (CA2–3)	1.62	0.01	0.21
Left hippocampal head (CA1)	0.20	0.00	0.66
Bilateral hippocampal body–tail (CA2–3)	0.31	0.00	0.58
Right hippocampal tail (CA1–3)— Bilateral hippocampal head–body (dentate gyrus-CA4)	1.31	0.01	0.25
Bilateral hippocampal body–tail (CA1)	2.61	0.02	0.11

Age, sex and years of education were set as covariates. An asterisk indicates significance after Bonferroni correction.

Intra-network abnormality in major depression

The correlations among age and loading coefficients of seven intra-networks in HS and major depressive disorder were shown in the correlation matrix (Supplementary Fig. 1). Table 3 shows the results of MANCOVA. There was a significant difference in the bilateral hippocampal tail (CA1–3) network ($P = 0.004$, $\eta p^2 = 0.05$).

In a binomial logistic regression analysis, bilateral networks, including the bilateral hippocampal tail (CA1–3) and bilateral hippocampal body–tail (CA2–3) were significant predictors for major depressive disorder ($P = 0.00002$, 0.001 , respectively) (Table 4). When the cut-off value was set to 0.5 with the equation obtained from the regression analysis, the sensitivity, specificity and accuracy were 84.6, 71.4 and 78.1%, respectively. In the ROC analysis, the area under the curve was 0.83 (Fig. 4).

Discussion

The examination of the intrinsic connectivity of each voxel in the hippocampus revealed two major results. First, multiple networks connecting the bilateral hippocampi were described, not only in the ipsilateral hippocampus. Second, major depressive disorder showed a significant difference in the networks connecting the bilateral hippocampal tails (CA1–3). In addition, the bilateral hippocampal networks are predictors of major depressive disorder. To the best of our knowledge, this is the first study to assess intra-network abnormalities in the hippocampi of patients with major depressive disorder.

Table 4 Binominal logistic regression model for predicting MDD

	OR	Lower CI	Upper CI	P
Bilateral hippocampal tail (CA1–3)	3.62	2.01	6.52	0.00002*
Right hippocampal head (subiculum, CA1)	0.53	0.27	1.02	0.06
Right hippocampal body (CA2–3)	1.38	0.90	2.13	0.14
Left hippocampal head (CA1)	1.15	0.59	2.26	0.68
Bilateral hippocampal body–tail (CA2–3)	0.30	0.15	0.60	0.001*
Right hippocampal tail (CA1–3)— Bilateral hippocampal head–body (dentate gyrus-CA4)	0.57	0.35	0.92	0.02
Bilateral hippocampal body–tail (CA1)	1.90	1.14	3.14	0.01

An asterisk indicates significance after Bonferroni correction.
CI = confidence interval; OR = odds ratio.

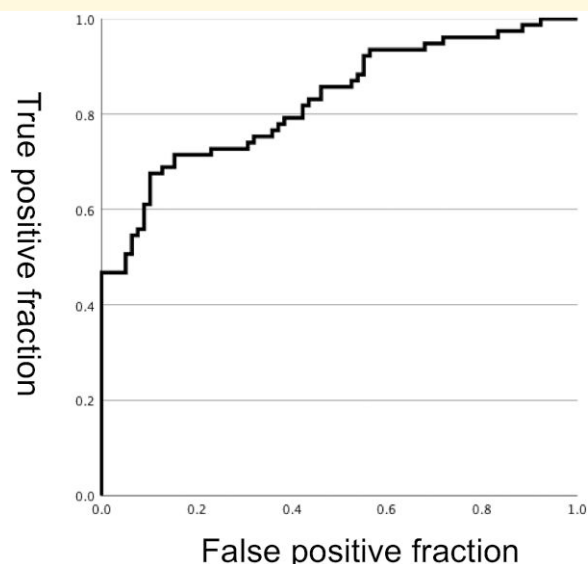


Figure 4 ROC curve. Receiver operating characteristic curves for performance of logistic regression to predict major depressive patients using the intra-networks in the hippocampus. The area under the curve was 0.83. When the cut-off value was set to 0.5 with the equation obtained from the regression analysis, the sensitivity, specificity and accuracy were 84.6, 71.4 and 78.1%, respectively.

Intra-network in the hippocampus using MRI

While many studies have investigated non-uniform structural changes using hippocampal subfield segmentation, MRI studies of the intra-network in the hippocampus are still developing. In the HSs, the intra-network was described using resting-state functional images of ~1.5 mm isotropic³⁴⁻³⁶ and 3.0 mm isotropic³⁷ voxels on 3T MRI and 1.5–2.0 mm isotropic voxels

on 7T MRI^{8,38} combined with hippocampal subfields segmentation from structural imaging. In these previous studies, functional networks of bilateral⁸ and along the longitudinal axis³⁸ were found, consistent with the structural covariance networks in this study. Regarding intra-network alterations in the hippocampus, age-related dysfunction in the network along the longitudinal axis was observed.^{36,39} Furthermore, the network along the longitudinal axis may contribute to memory decline.³⁶

In this study, we extracted the intra-networks in the hippocampus based on SBM and ICA. SBM and ICA consider information across different voxels and extract naturally occurring covariance patterns. This data-driven method examines the connectivity of each voxel without prior identification of the hippocampal subfields. In addition, a previous study on cross-modal integration focused on the structural covariance and resting-state functional network revealed that structural covariance networks are more likely to reflect short-distance connections.⁴⁰ Because the intra-network in the hippocampus contains very short-distance connections, such as synapse connections, the method presented in this study is considered suitable for evaluating the intra-network in the hippocampus.

Major depression disorder and intra-network in the hippocampus

Accumulating evidence indicates that major depressive disorder shows structural and functional changes in the hippocampus^{41,42} and large-scale network dysfunction across the brain on resting-state functional MRI.^{43,44} Regarding structural changes in the hippocampus, subfield-specific changes are considered to exist.⁴⁵⁻⁴⁷ However, findings on subfield-specific changes in major depressive disorders are inconsistent because they may depend not only on medication use⁴⁸ and illness duration⁴⁹ but also on the diversity of segmentation protocols.¹⁰ Regarding hippocampal network abnormality in major depressive disorder, recent studies have focused on the connectivity of specific hippocampal subfields with the rest of the brain.^{50,51} For instance, it has been reported that a disturbed functional network between the right anterior hippocampus and insula correlates with the symptoms of depression in major depressive disorder.⁵⁰

Furthermore, bilateral intra-networks in the hippocampus have been shown to predict major depressive disorder. In this study, we found disturbed bilateral hippocampal tail (CA1-3) networks in patients with major depressive disorder. However, there were no significant differences in the networks along the longitudinal axis. Although recent findings have highlighted the network along the longitudinal axis as a key contributor to the functional organization,^{52,53} the underlying function of bilateral networks remains unclear. Interestingly, a recent study separated the structural and functional networks into two models: (i) bilateral hippocampal formations and (ii) bilateral extra-hippocampal structures by mapping networks of the medial temporal lobe using graph theory and hippocampal subfield segmentation on 7T MRI.⁸ Thus, both the ICA based on each voxel and graph theory based on hippocampal subfields revealed

bilateral networks. Future research on the bilateral hippocampal networks found by new analysis methods is needed to reveal their role in brain function and psychiatric disorders. The finding of lateralized morphometric changes of the hippocampus in major depressive disorder^{54,55} may be related to the bilateral network in the hippocampus.

Study limitations

A limitation of our study is that functional MRI was not performed to confirm the intra-network in the hippocampus extracted from the structural MRI. However, a previous study showed a direct association between functional networks and structural covariance networks using SBM across the entire brain.¹⁵ Furthermore, in the intra-network in the hippocampus based on hippocampal subfield segmentation, a correlation between structural and functional networks has been reported.⁸

Conclusion

We present a novel method for evaluating voxel-based structural covariance networks within the hippocampus. One advantage of this method is that a detailed network can be estimated using conventional structural imaging. In addition, we found novel networks in the bilateral hippocampus that were disturbed in patients with major depressive disorder. Furthermore, the bilateral networks in the hippocampus could predict major depressive disorders (MDD).

Funding

This work was supported by Japan Society for the Promotion of Science KAKENHI (grant number JP19k17214).

Competing interests

The authors report no competing interests.

Data availability

The data that support the findings of this study are available from the corresponding author, upon reasonable request.

Supplementary material

Supplementary material is available at *Brain Communications* online.

References

- Schmaal L, Veltman DJ, van Erp TG, et al. Subcortical brain alterations in major depressive disorder: Findings from the ENIGMA major depressive disorder working group. *Mol Psychiatry*. 2015;21(6):806-812.

- Campbell S, Marriott M, Nahmias C, MacQueen GM. Lower hippocampal volume in patients suffering from depression: A meta-analysis. *Am J Psychiatry*. 2004;161(4):598-607.
- Kempton MJ, Salvador Z, Munafo MR, et al. Structural neuroimaging studies in major depressive disorder. Meta-analysis and comparison with bipolar disorder. *Arch Gen Psychiatry*. 2011;68(7):675-690.
- Chen MC, Hamilton JP, Gotlib IH. Decreased hippocampal volume in healthy girls at risk of depression. *Arch Gen Psychiatry*. 2010;67(3):270-276.
- Brown ES, Hughes CW, McColl R, Peshock R, King KS, Rush AJ. Association of depressive symptoms with hippocampal volume in 1936 adults. *Neuropsychopharmacology*. 2014;39(3):770-779.
- Kotkowski E, Price LR, Mickle Fox P, Vanasse TJ, Fox PT. The hippocampal network model: A transdiagnostic metaconnectomic approach. *Neuroimage Clin*. 2018;18:115-129.
- Aggleton JP. Multiple anatomical systems embedded within the primate medial temporal lobe: Implications for hippocampal function. *Neurosci Biobehav Rev*. 2012;36(7):1579-1596.
- Shah P, Bassett DS, Wisse LEM, et al. Mapping the structural and functional network architecture of the medial temporal lobe using 7T MRI. *Hum Brain Mapp*. 2018;39(2):851-865.
- de Flores R, Mutlu J, Bejanin A, et al. Intrinsic connectivity of hippocampal subfields in normal elderly and mild cognitive impairment patients. *Hum Brain Mapp*. 2017;38(10):4922-4932.
- Wisse LEM, Daugherty AM, Olsen RK, et al. A harmonized segmentation protocol for hippocampal and parahippocampal subregions: Why do we need one and what are the key goals? *Hippocampus*. 2017;27(1):3-11.
- Wisse LE, Biessels GJ, Geerlings MI. A critical appraisal of the hippocampal subfield segmentation package in FreeSurfer. *Front Aging Neurosci*. 2014;6:261.
- Watanabe K, Kakeda S, Katsuki A, et al. Whole-brain structural covariance network abnormality in first-episode and drug-naïve major depressive disorder. *Psychiatry Res Neuroimaging*. 2020;300:111083.
- Evans AC. Networks of anatomical covariance. *Neuroimage*. 2013;80:489-504.
- Luo L, Xu L, Jung R, Pearlson G, Adali T, Calhoun VD. Constrained source-based morphometry identifies structural networks associated with default mode network. *Brain Connect*. 2012;2(1):33-43.
- Segall JM, Allen EA, Jung RE, et al. Correspondence between structure and function in the human brain at rest. *Front Neuroinform*. 2012;6:10.
- Xu L, Groth KM, Pearlson G, Schretlen DJ, Calhoun VD. Source-based morphometry: The use of independent component analysis to identify gray matter differences with application to schizophrenia. *Hum Brain Mapp*. 2009;30(3):711-724.
- Turner JA, Calhoun VD, Michael A, et al. Heritability of multivariate gray matter measures in schizophrenia. *Twin Res Hum Genet*. 2012;15(3):324-335.
- Hamilton M. Development of a rating scale for primary depressive illness. *Br J Soc Clin Psychol*. 1967;6(4):278-296.
- Jovicich J, Czanner S, Greve D, et al. Reliability in multi-site structural MRI studies: Effects of gradient non-linearity correction on phantom and human data. *Neuroimage*. 2006;30(2):436-443.
- Sled JG, Zijdenbos AP, Evans AC. A nonparametric method for automatic correction of intensity nonuniformity in MRI data. *IEEE Trans Med Imaging*. 1998;17(1):87-97.
- Ashburner J. A fast diffeomorphic image registration algorithm. *Neuroimage*. 2007;38(1):95-113.
- Ashburner J. SPM: A history. *Neuroimage*. 2012;62(2):791-800.
- Ashburner J. Computational anatomy with the SPM software. *Magn Reson Imaging*. 2009;27(8):1163-1174.
- Tzourio-Mazoyer N, Landeau B, Papathanassiou D, et al. Automated anatomical labeling of activations in SPM using a

- macroscopic anatomical parcellation of the MNI MRI single-subject brain. *Neuroimage*. 2002;15(1):273-289.
25. Maldjian JA, Laurienti PJ, Burdette JH. Precentral gyrus discrepancy in electronic versions of the Talairach atlas. *Neuroimage*. 2004;21(1):450-455.
 26. Maldjian JA, Laurienti PJ, Kraft RA, Burdette JH. An automated method for neuroanatomic and cytoarchitectonic atlas-based interrogation of fMRI data sets. *Neuroimage*. 2003;19(3):1233-1239.
 27. Bell AJ, Sejnowski TJ. An information-maximization approach to blind separation and blind deconvolution. *Neural Comput*. 1995;7(6):1129-1259.
 28. Himberg J, Hyvärinen A, Esposito F. Validating the independent components of neuroimaging time series via clustering and visualization. *Neuroimage*. 2004;22(3):1214-1222.
 29. Yoon YB, Shin WG, Lee TY, et al. Brain structural networks associated with intelligence and visuomotor ability. *Sci Rep*. 2017;7(1):2177.
 30. Gupta CN, Calhoun VD, Rachakonda S, et al. Patterns of gray matter abnormalities in schizophrenia based on an international mega-analysis. *Schizophr Bull*. 2015;41(5):1133-1142.
 31. Grecucci A, Rubicondo D, Siugzdaite R, Surian L, Job R. Uncovering the social deficits in the autistic brain. A source-based morphometric study. *Front Neurosci*. 2016;10:388.
 32. Ciarochi JA, Calhoun VD, Lourens S, et al. Patterns of co-occurring gray matter concentration loss across the Huntington disease prodrome. *Front Neurol*. 2016;7:147.
 33. Dalton MA, Zeidman P, Barry DN, Williams E, Maguire EA. Segmenting subregions of the human hippocampus on structural magnetic resonance image scans: An illustrated tutorial. *Brain Neurosci Adv*. 2017;1:2398212817701448.
 34. Lacy JW, Stark CE. Intrinsic functional connectivity of the human medial temporal lobe suggests a distinction between adjacent MTL cortices and hippocampus. *Hippocampus*. 2012;22(12):2290-2302.
 35. Dalton MA, McCormick C, Maguire EA. Differences in functional connectivity along the anterior-posterior axis of human hippocampal subfields. *Neuroimage*. 2019;192:38-51.
 36. Stark SM, Frithsen A, Stark CEL. Age-related alterations in functional connectivity along the longitudinal axis of the hippocampus and its subfields. *Hippocampus*. 2021;31(1):11-27.
 37. Das SR, Pluta J, Mancuso L, Kliot D, Yushkevich PA, Wolk DA. Anterior and posterior MTL networks in aging and MCI. *Neurobiol Aging*. 2015;36(Suppl 1(0 1)):S141-S150.e1.
 38. Ezama L, Hernández-Cabrera JA, Seoane S, Pereda E, Janssen N. Functional connectivity of the hippocampus and its subfields in resting-state networks. *Eur J Neurosci*. 2021;53(10):3378-3393.
 39. Li X, Li Q, Wang X, Li D, Li S. Differential age-related changes in structural covariance networks of human anterior and posterior hippocampus. *Front Physiol*. 2018;9:518.
 40. Alexander-Bloch A, Raznahan A, Bullmore E, Giedd J. The convergence of maturational change and structural covariance in human cortical networks. *J Neurosci*. 2013;33(7):2889-2899.
 41. Milne AM, MacQueen GM, Hall GB. Abnormal hippocampal activation in patients with extensive history of major depression: An fMRI study. *J Psychiatry Neurosci*. 2012;37(1):28-36.
 42. Schmitter D, Roche A, Marechal B, et al. An evaluation of volume-based morphometry for prediction of mild cognitive impairment and Alzheimer's disease. *Neuroimage Clin*. 2015;7:7-17.
 43. Gong Q, He Y. Depression, neuroimaging and connectomics: A selective overview. *Biol Psychiatry*. 2015;77(3):223-235.
 44. Kaiser RH, Andrews-Hanna JR, Wager TD, Pizzagalli DA. Large-scale network dysfunction in major depressive disorder: A meta-analysis of resting-state functional connectivity. *JAMA Psychiatry*. 2015;72(6):603-611.
 45. Cao B, Passos IC, Mwangi B, et al. Hippocampal subfield volumes in mood disorders. *Mol Psychiatry*. 2017;22(9):1352-1358.
 46. Watanabe R, Kakeda S, Watanabe K, et al. Relationship between the hippocampal shape abnormality and serum cortisol levels in first-episode and drug-naïve major depressive disorder patients. *Depress Anxiety*. 2017;34(5):401-409.
 47. Han KM, Kim A, Kang W, et al. Hippocampal subfield volumes in major depressive disorder and bipolar disorder. *Eur Psychiatry*. 2019;57:70-77.
 48. Katsuki A, Watanabe K, Nguyen L, et al. Structural changes in hippocampal subfields in patients with continuous remission of drug-naïve major depressive disorder. *Int J Mol Sci*. 2020;21(9):3032.
 49. Treadway MT, Waskom ML, Dillon DG, et al. Illness progression, recent stress, and morphometry of hippocampal subfields and medial prefrontal cortex in major depression. *Biol Psychiatry*. 2015;77(3):285-294.
 50. Hu J, Liu J, Liu Y, et al. Dysfunction of the anterior and intermediate hippocampal functional network in major depressive disorders across the adult lifespan. *Biol Psychol*. 2021;165:108192.
 51. Shengli C, Yingli Z, Zheng G, et al. An aberrant hippocampal sub-regional network, rather than structure, characterizes major depressive disorder. *J Affect Disord*. 2022;302:123-130.
 52. Strange BA, Witter MP, Lein ES, Moser EI. Functional organization of the hippocampal longitudinal axis. *Nat Rev Neurosci*. 2014;15(10):655-669.
 53. Genov S, Bernhardt BC, La Joie R, Amunts K, Eickhoff SB. The many dimensions of human hippocampal organization and (dys)function. *Trends Neurosci*. 2021;44(12):977-989.
 54. Nifosi F, Toffanin T, Follador H, et al. Reduced right posterior hippocampal volume in women with recurrent familial pure depressive disorder. *Psychiatry Res*. 2010;184(1):23-28.
 55. Jaworska N, Yücel K, Courtright A, MacMaster FP, Sembo M, MacQueen G. Subgenual anterior cingulate cortex and hippocampal volumes in depressed youth: The role of comorbidity and age. *J Affect Disord*. 2016;190:726-732.